



TREATMENT OF RANK DEFICIENCY IN ACOUSTICS USING SVD

J. T. CHEN*

*Department of Harbor and River Engineering
National Taiwan Ocean University
P. O. Box 7-59, Keelung 2024, Taiwan
jtchen@mail.ntou.edu.tw*

I. L. CHEN

*Department of Naval Architecture
National Kaohsiung Marine University, Kaohsiung, Taiwan*

K. H. CHEN

*Department of Information Management
Toko University, Chia-Yi, Taiwan*

Received 25 January 2002

Revised 15 January 2005

In this paper, we proposed a unified formulation to explain the reason why spurious eigensolution occurs in the eigenproblem of interior acoustics using the real-part and imaginary-part BEMs and why fictitious frequency occurs in exterior acoustics using the complex-valued BEM. Both the two problems stem from the rank deficiency of the influence matrix. Based on the circulant properties and degenerate kernels, an analytical study in a discrete system for a circular cavity is conducted. The Fredholm alternative theorem is employed to study the rank-deficiency problems in conjunction with singular value decomposition updating technique. The spurious and fictitious boundary modes are found to locate in the column vectors of left unitary matrix. Also, the effects of different types of boundary condition on the spurious and fictitious solutions using direct and indirect methods are discussed. The mathematical and physical meanings for the nontrivial boundary solution in spurious eigensolution and fictitious frequency are explained. Numerical experiments are found to agree with the analytical predictions.

Keywords: Rank deficiency; circulant; degenerate kernel; BEM; spurious eigenvalue; fictitious frequency.

1. Introduction

Acoustic problems are generally modeled using the wave equation in the time domain. For harmonic excitation, it can be transformed to the Helmholtz equation in the frequency domain. Integral equations have been utilized to solve the interior and exterior acoustic

*Corresponding author.

problems for a long time. While the solution to the original boundary value problem in the exterior domain to the boundary is perfectly unique for all wave numbers, this is not the case for the numerical treatment of integral equation formulation, which breaks down at certain frequencies known as irregular frequencies or fictitious frequencies. This problem is completely nonphysical because there are no discrete eigenvalues for the exterior problems. It is well known that the singular (*UT*) equation results in fictitious frequencies which are associated with the interior acoustic frequency with essential homogeneous boundary conditions, while the hypersingular (*LM*) equation produces fictitious frequencies which are associated with natural homogeneous boundary conditions.¹ The general derivation was provided in a continuous system,¹ and a discrete system was analytically studied using a circulant.² Schenck³ proposed a CHIEF (Combined Helmholtz Interior integral Equation Formulation) method, which is easy to implement and is efficient but still has some drawbacks. Burton and Miller⁴ proposed an integral equation that was valid for all wave numbers by forming a linear combination of the singular integral equation and its normal derivative through an imaginary constant. In case of a fictitious frequency, the resulting coefficient matrix for the exterior acoustic problems becomes ill-conditioned. This means that the boundary integral equations are not linearly independent and the resulted matrix is rank deficient. In the fictitious-frequency case, the rank of the coefficient matrix is less than $2N$, where $2N$ is the number of the boundary unknowns. The SVD (Singular Value Decomposition) updating technique can be employed to detect fictitious frequencies by checking whether the first minimum singular value, σ_1 , is zero or not.⁵

For interior problems, eigensolutions are very important bases in vibrations and acoustics. Based on the complex-valued boundary element method,⁶ the eigenvalues and eigenmodes can be determined. Nevertheless, complex arithmetic is required. To avoid complex arithmetic, many approaches, the multiple reciprocity method (MRM),⁷ real-part and imaginary-part BEMs^{8,9} have been proposed. For example, Tai and Shaw¹⁰ employed only real-part kernel in integral formulation. A simplified method using only the real-part or imaginary-part kernel was also presented by De Mey.⁸ Although De Mey found that the zeros for a real-part of the complex determinant may be different from those for real-part or imaginary-part determinant, the spurious eigensolutions were not discovered analytically. Chen and Wong¹¹ found the spurious eigensolutions analytically in MRM using a simple example. Later, Kamiya *et al.*¹² and Yeih *et al.*¹³ independently claimed that MRM is no more than the real-part BEM. Kang *et al.*¹⁴ employed the Nondimensional Dynamic Influence Function method (NDIF) to solve the eigenproblem. Chen *et al.*¹⁵ commented that the NDIF method is a special case of imaginary-part BEM. Kang and Lee¹⁶ also found the spurious eigensolutions and filtered out the spurious eigenvalues by using the net approach. The reason why spurious eigenvalues occur in the real-part BEM is the loss of the constraints, which was investigated by Yeih *et al.*¹³ The spurious eigensolutions and fictitious solutions arise from an improper approximation of the null space of operator.¹⁷ The fewer number of constraint equations makes the solution space larger. The spurious eigensolutions can be filtered out by using many alternatives, e.g., the complex-valued formulation, the domain partition technique,¹⁸ the dual formulation in conjunction with the SVD updating

techniques¹⁹ and the CHEEF (Combined Helmholtz Exterior integral Equation Formulation) method.²⁰

One of the important and basic tools of modern numerical analysis; particularly linear algebra for science and engineering, is SVD. The SVD technique is a form of orthogonal matrix factorization that is more powerful than the QR factorization, although SVD is not often included in introductory courses.²¹ Especially, it is more versatile for the ill-posed system.²² The present paper is but one of many fields of application and it is likely that within five or ten years, SVD will become one of the most fundamental tools for the engineering community, particularly in the case of linear system. It is interesting that SVD updating technique as well as downdating technique have been applied to data retrieval.²³

Based on the circulant properties and degenerate kernels, the reason why the fictitious wave number and spurious eigensolution occur can be easily understood in this paper. We explore the mechanism of them and found the relationship between the spurious eigenvalue (interior problem) and fictitious frequency (exterior problem). The Fredholm alternative theorem in conjunction with SVD updating technique will be employed to study the mathematical structure of the influence matrices. The spurious and fictitious solutions for problems subject to different boundary conditions using direct and indirect methods will be investigated. Numerical examples will be demonstrated for the theoretical study.

2. A Unified Integral Formulation for the Interior and Exterior Acoustic Problems

The governing equation for acoustics is the Helmholtz equation as follows:

$$\nabla^2 u(\mathbf{x}) + k^2 u(\mathbf{x}) = 0, \quad \mathbf{x} \in D, \quad (1)$$

where u is the acoustic potential, ∇^2 is the Laplacian operator, D can be D^i for the interior problem and D^e for the exterior problem and k is the wave number, which is the angular frequency over the speed of sound.

2.1. Direct method: Singular (UT) or hypersingular (LM) equation

Based on the dual formulation, the unified null-field integral formulation for the Helmholtz equation using the direct method can be written as

$$0 = \int_B T(\mathbf{s}, \mathbf{x}) u(\mathbf{s}) dB(\mathbf{s}) - \int_B U(\mathbf{s}, \mathbf{x}) t(\mathbf{s}) dB(\mathbf{s}), \quad (2)$$

$$0 = \int_B M(\mathbf{s}, \mathbf{x}) u(\mathbf{s}) dB(\mathbf{s}) - \int_B L(\mathbf{s}, \mathbf{x}) t(\mathbf{s}) dB(\mathbf{s}), \quad (3)$$

where \mathbf{x} is a field point and \mathbf{s} is a source point, $t(\mathbf{s}) = \partial u(\mathbf{s})/\partial n_{\mathbf{s}}$, $U(\mathbf{s}, \mathbf{x})$ is the fundamental solution, $T(\mathbf{s}, \mathbf{x}) = \partial U(\mathbf{s}, \mathbf{x})/\partial n_{\mathbf{s}}$, $L(\mathbf{s}, \mathbf{x}) = \partial U(\mathbf{s}, \mathbf{x})/\partial n_{\mathbf{x}}$ and $M(\mathbf{s}, \mathbf{x}) = \partial^2 U(\mathbf{s}, \mathbf{x})/\partial n_{\mathbf{s}} \partial n_{\mathbf{x}}$, B denotes the boundary enclosing D . For the exterior problem, we have $U = U^i(\mathbf{s}, \mathbf{x})$, $T = T^i(\mathbf{s}, \mathbf{x})$, $L = L^i(\mathbf{s}, \mathbf{x})$ and $M = M^i(\mathbf{s}, \mathbf{x})$. In case of interior problem, we

have $U = U^e(\mathbf{s}, \mathbf{x})$, $T = T^e(\mathbf{s}, \mathbf{x})$, $L = L^e(\mathbf{s}, \mathbf{x})$ and $M = M^e(\mathbf{s}, \mathbf{x})$. The selected kernels are designed to have the null-field equation without jump terms. The eight kernels of U^i , U^e , T^i , \dots and M^e can be obtained by using the degenerate kernels.² The explicit forms of the four kernels will be elaborated on later.

2.2. Indirect method: Single-layer (UL) or double-layer (TM) approaches

By employing the indirect method of single-layer (UL) and double-layer (TM) approaches, we have

$$u(\mathbf{x}) = \int_{B'} U(\mathbf{s}, \mathbf{x}) \phi(\mathbf{s}) dB(\mathbf{s}), \quad \text{single layer approach,} \quad (4)$$

$$t(\mathbf{x}) = \int_{B'} L(\mathbf{s}, \mathbf{x}) \phi(\mathbf{s}) dB(\mathbf{s}), \quad \text{single layer approach,} \quad (5)$$

and

$$u(\mathbf{x}) = \int_{B'} T(\mathbf{s}, \mathbf{x}) \psi(\mathbf{s}) dB(\mathbf{s}), \quad \text{double layer approach,} \quad (6)$$

$$t(\mathbf{x}) = \int_{B'} M(\mathbf{s}, \mathbf{x}) \psi(\mathbf{s}) dB(\mathbf{s}), \quad \text{double layer approach,} \quad (7)$$

where B' is an auxiliary boundary, ϕ and ψ are the fictitious densities of single-layer and double-layer potentials, respectively. In the indirect method, we can superimpose the fictitious densities of single-layer or double-layer potential on the fictitious boundary with a radius R , and collocating the field point along the real boundary with a radius ρ . In the exterior problem, we have $R < \rho$. ($R > \rho$ for the interior problem). For the exterior problem, we have $U = U^e(\mathbf{s}, \mathbf{x})$, $T = T^e(\mathbf{s}, \mathbf{x})$, $L = L^e(\mathbf{s}, \mathbf{x})$ and $M = M^e(\mathbf{s}, \mathbf{x})$. In case of interior problem, we have $U = U^i(\mathbf{s}, \mathbf{x})$, $T = T^i(\mathbf{s}, \mathbf{x})$, $L = L^i(\mathbf{s}, \mathbf{x})$ and $M = M^i(\mathbf{s}, \mathbf{x})$.

3. Analytical Study for Spurious and Fictitious Solutions in BEM using Degenerate Kernels and Circulants

By using the two bases of the first and the second-kind Bessel functions of the n th order and their derivatives, $J_n(kx)$, $J'_n(kx)$, $Y_n(kx)$ and $Y'_n(kx)$, we can decompose the two-dimensional kernel functions into

$$U(\mathbf{s}, \mathbf{x}) = \begin{cases} U^i(R, \theta; \rho, 0) = \sum_{n=-\infty}^{n=\infty} \frac{\pi}{2} [-iJ_n(kR) + Y_n(kR)] J_n(k\rho) \cos(n\theta), & R > \rho, \\ U^e(R, \theta; \rho, 0) = \sum_{n=-\infty}^{n=\infty} \frac{\pi}{2} [-iJ_n(k\rho) + Y_n(k\rho)] J_n(kR) \cos(n\theta), & R < \rho, \end{cases} \quad (8)$$

$$T(\mathbf{s}, \mathbf{x}) = \begin{cases} T^i(R, \theta; \rho, 0) = \sum_{n=-\infty}^{n=\infty} \frac{k\pi}{2} [-iJ'_n(kR) + Y'_n(kR)] J_n(k\rho) \cos(n\theta), & R > \rho, \\ T^e(R, \theta; \rho, 0) = \sum_{n=-\infty}^{n=\infty} \frac{k\pi}{2} [-iJ_n(k\rho) + Y_n(k\rho)] J'_n(kR) \cos(n\theta), & R < \rho, \end{cases} \quad (9)$$

$$L(\mathbf{s}, \mathbf{x}) = \begin{cases} L^i(R, \theta; \rho, 0) = \sum_{n=-\infty}^{n=\infty} \frac{k\pi}{2} [-iJ_n(kR) + Y_n(kR)] J'_n(k\rho) \cos(n\theta), & R > \rho, \\ L^e(R, \theta; \rho, 0) = \sum_{n=-\infty}^{n=\infty} \frac{k\pi}{2} [-iJ'_n(k\rho) + Y'_n(k\rho)] J_n(kR) \cos(n\theta), & R < \rho, \end{cases} \quad (10)$$

$$M(\mathbf{s}, \mathbf{x}) = \begin{cases} M^i(R, \theta; \rho, 0) = \sum_{n=-\infty}^{n=\infty} \frac{k^2\pi}{2} [-iJ'_n(kR) + Y'_n(kR)] J'_n(k\rho) \cos(n\theta), & R > \rho, \\ M^e(R, \theta; \rho, 0) = \sum_{n=-\infty}^{n=\infty} \frac{k^2\pi}{2} [-iJ'_n(k\rho) + Y'_n(k\rho)] J'_n(kR) \cos(n\theta), & R < \rho, \end{cases} \quad (11)$$

where $i^2 = -1$, $\mathbf{s} = (R, \theta)$ and \mathbf{x} can be specified by $(\rho, 0)$ in the polar coordinate without loss of generality. The definitions of ρ , R and θ for the interior problem using the direct and indirect methods are shown in Figs. 1 and 2, respectively. For the exterior problems, they are shown in Figs. 3 and 4, respectively. Based on the circulants for the finite number degrees of freedom (d.o.f.) system by uniformly discretizing $2N$ constant elements for a circular boundary, we have the influence matrix

$$[G] = \begin{bmatrix} a_0 & a_1 & a_2 & \cdots & a_{2N-2} & a_{2N-1} \\ a_{2N-1} & a_0 & a_1 & \cdots & a_{2N-3} & a_{2N-2} \\ a_{2N-2} & a_{2N-1} & a_0 & \cdots & a_{2N-4} & a_{2N-3} \\ \vdots & \vdots & \vdots & \ddots & \vdots & \vdots \\ a_1 & a_2 & a_3 & \cdots & a_{2N-1} & a_0 \end{bmatrix}, \quad (12)$$

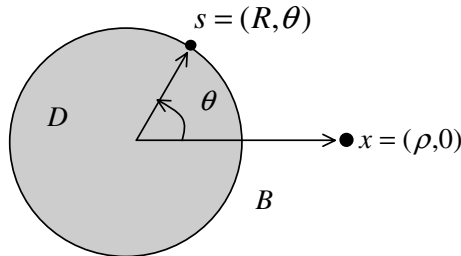


Fig. 1. The definitions of ρ , R and θ , for the interior problem using the direct method.

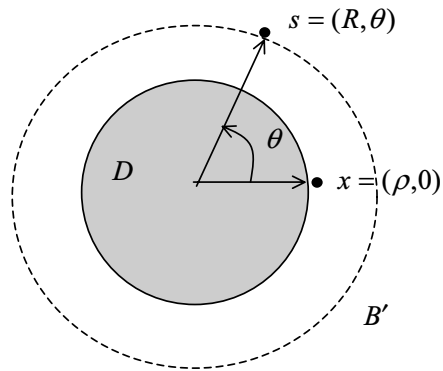


Fig. 2. The definitions of ρ , R and θ , for the interior problem using the indirect method.

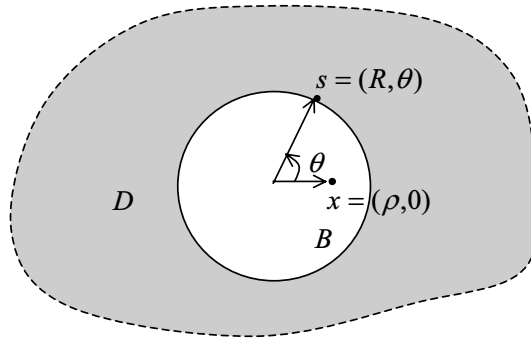


Fig. 3. The definitions of ρ , R and θ , for the exterior problem using the direct method.

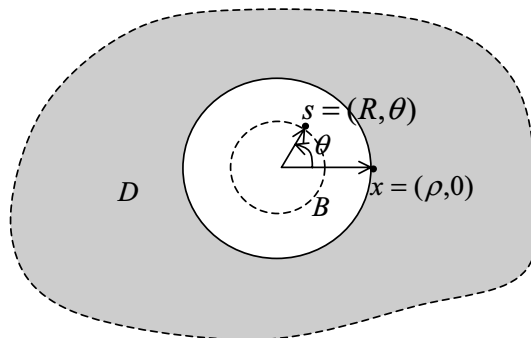


Fig. 4. The definitions of ρ , R and θ , for the exterior problem using the indirect method.

where

$$a_m = \int_{(m-\frac{1}{2})\Delta\theta}^{(m+\frac{1}{2})\Delta\theta} G(R, \theta; \rho, 0) R d\theta \approx G(R, \theta_m; \rho, 0) R \Delta\theta, \quad m = 0, 1, 2, \dots, 2N - 1 \quad (13)$$

in which $m = 0, 1, 2, \dots, 2N - 1$. $\Delta\theta = (2\pi/2N)$, $\theta_m = m\Delta\theta$ and $G(R, \theta; \rho, 0)$ can be U^i , U^e , T^i , T^e , L^i , L^e , M^i or M^e . By using the similar properties for the eight circulants, we have

$$\det[U^i] = \lambda_0 \lambda_N (\lambda_1 \lambda_2 \cdots \lambda_{N-1}) (\lambda_{-1} \lambda_{-2} \cdots \lambda_{-(N-1)}), \quad (14)$$

$$\det[U^e] = \lambda_0 \lambda_N (\lambda_1 \lambda_2 \cdots \lambda_{N-1}) (\lambda_{-1} \lambda_{-2} \cdots \lambda_{-(N-1)}), \quad (15)$$

$$\det[T^e] = \mu_0 \mu_N (\mu_1 \mu_2 \cdots \mu_{N-1}) (\mu_{-1} \mu_{-2} \cdots \mu_{-(N-1)}), \quad (16)$$

$$\det[L^i] = \mu_0 \mu_N (\mu_1 \mu_2 \cdots \mu_{N-1}) (\mu_{-1} \mu_{-2} \cdots \mu_{-(N-1)}), \quad (17)$$

$$\det[T^i] = \nu_0 \nu_N (\nu_1 \nu_2 \cdots \nu_{N-1}) (\nu_{-1} \nu_{-2} \cdots \nu_{-(N-1)}), \quad (18)$$

$$\det[L^e] = \nu_0 \nu_N (\nu_1 \nu_2 \cdots \nu_{N-1}) (\nu_{-1} \nu_{-2} \cdots \nu_{-(N-1)}), \quad (19)$$

$$\det[M^i] = \kappa_0 \kappa_N (\kappa_1 \kappa_2 \cdots \kappa_{N-1}) (\kappa_{-1} \kappa_{-2} \cdots \kappa_{-(N-1)}), \quad (20)$$

$$\det[M^e] = \kappa_0 \kappa_N (\kappa_1 \kappa_2 \cdots \kappa_{N-1}) (\kappa_{-1} \kappa_{-2} \cdots \kappa_{-(N-1)}), \quad (21)$$

where

$$\lambda_\ell = \pi^2 \rho [-iJ_\ell(k\rho) + Y_\ell(k\rho)] J_\ell(k\rho), \quad \ell = 0, \pm 1, \pm 2, \dots, \pm(N-1), N, \quad (22)$$

$$\mu_\ell = \pi^2 k \rho [-iJ_\ell(k\rho) + Y_\ell(k\rho)] J'_\ell(k\rho), \quad \ell = 0, \pm 1, \pm 2, \dots, \pm(N-1), N, \quad (23)$$

$$\nu_\ell = \pi^2 k \rho [-iJ'_\ell(k\rho) + Y'_\ell(k\rho)] J_\ell(k\rho), \quad \ell = 0, \pm 1, \pm 2, \dots, \pm(N-1), N, \quad (24)$$

$$\kappa_\ell = \pi^2 k^2 \rho [-iJ'_\ell(k\rho) + Y'_\ell(k\rho)] J'_\ell(k\rho), \quad \ell = 0, \pm 1, \pm 2, \dots, \pm(N-1), N, \quad (25)$$

in which the singularity is distributed on the boundary such that $R = \rho$.

4. Fictitious Values for Exterior Problems using BEM

4.1. Direct method: Singular (UT) or hypersingular (LM) equation

For the radiation problem subject to the Dirichlet boundary condition, $u(\mathbf{x}) = \bar{u}$ is considered on the boundary. By employing the singular (UT) and hypersingular (LM) formulations for the circular radiator, we obtain the following dual equations,

$$[U^i]\{t\} = [T^i]\{\bar{u}\}, \quad (26)$$

$$[L^i]\{t\} = [M^i]\{\bar{u}\}. \quad (27)$$

Based on Eqs. (22) and (26), and Eqs. (23) and (27), the possible fictitious frequencies occur at the position where k satisfies

$$UT: [-iJ_\ell(k\rho) + Y_\ell(k\rho)] J_\ell(k\rho) = 0, \quad \ell = 0, \pm 1, \pm 2, \dots, \pm(N-1), N, \quad (28)$$

$$LM: [-iJ_\ell(k\rho) + Y_\ell(k\rho)] J'_\ell(k\rho) = 0, \quad \ell = 0, \pm 1, \pm 2, \dots, \pm(N-1), N, \quad (29)$$

respectively. Since the term of $[-iJ_\ell(k\rho) + Y_\ell(k\rho)]$ is never zero for any value of k , the k value satisfying Eq. (28), implies

$$UT: \quad J_\ell(k\rho) = 0, \quad (30)$$

and the k value satisfying Eq. (29), implies

$$LM: \quad J'_\ell(k\rho) = 0. \quad (31)$$

For the Neumann radiation problem with $t(\mathbf{x}) = \bar{t}$ specified on the boundary, we can obtain the following equations,

$$[T^i]\{u\} = [U^i]\{\bar{t}\}, \quad (32)$$

$$[M^i]\{u\} = [L^i]\{\bar{t}\}. \quad (33)$$

Based on Eqs. (24) and (32), and Eqs. (25) and (33), the possible fictitious values occur at the position where k satisfies

$$UT: \quad [-iJ'_\ell(k\rho) + Y'_\ell(k\rho)]J_\ell(k\rho) = 0, \quad \ell = 0, \pm 1, \pm 2, \dots, \pm(N-1), N. \quad (34)$$

$$LM: \quad [-iJ'_\ell(k\rho) + Y'_\ell(k\rho)]J'_\ell(k\rho) = 0, \quad \ell = 0, \pm 1, \pm 2, \dots, \pm(N-1), N. \quad (35)$$

Since $[-iJ'_\ell(k\rho) + Y'_\ell(k\rho)]$ is never zero for any value of k , the k value satisfying Eq. (34), implies

$$UT: \quad J_\ell(k\rho) = 0, \quad (36)$$

and the k value satisfying Eq. (35), implies

$$LM: \quad J'_\ell(k\rho) = 0. \quad (37)$$

4.2. Indirect method: Single-layer (UL) or double-layer (TM) approach

By employing the indirect method of single-layer (UL) or double-layer (TM) approaches for the exterior radiation problem, we have

$$\{u\} = [U^e]\{\phi\}, \quad (38)$$

$$\{t\} = [L^e]\{\phi\}, \quad (39)$$

or

$$\{u\} = [T^e]\{\psi\}, \quad (40)$$

$$\{t\} = [M^e]\{\psi\}. \quad (41)$$

Considering the Dirichlet radiation problem with Eqs. (22) and (38), and Eqs. (23) and (40), the possible fictitious frequencies occur at the position where k satisfies

$$UL: \quad [-iJ_\ell(k\rho) + Y_\ell(k\rho)]J_\ell(k\rho) = 0, \quad \ell = 0, \pm 1, \pm 2, \dots, \pm(N-1), N, \quad (42)$$

$$TM: \quad [-iJ_\ell(k\rho) + Y_\ell(k\rho)]J'_\ell(k\rho) = 0, \quad \ell = 0, \pm 1, \pm 2, \dots, \pm(N-1), N, \quad (43)$$

respectively. The k value satisfying Eq. (42), implies

$$UL: \quad J_\ell(k\rho) = 0. \quad (44)$$

The k value satisfying Eq. (43), implies

$$TM: \quad J'_\ell(k\rho) = 0. \quad (45)$$

Considering the Neumann radiation problem with Eqs. (24) and (39), and Eqs. (25) and (41), the possible fictitious values occur at the position where k satisfies

$$UL: \quad [-iJ'_\ell(k\rho) + Y'_\ell(k\rho)]J_\ell(k\rho) = 0, \quad \ell = 0, \pm 1, \pm 2, \dots, \pm(N-1), N, \quad (46)$$

$$TM: \quad [-iJ'_\ell(k\rho) + Y'_\ell(k\rho)]J'_\ell(k\rho) = 0, \quad \ell = 0, \pm 1, \pm 2, \dots, \pm(N-1), N, \quad (47)$$

respectively. The k value satisfying Eq. (46), implies

$$UL: \quad J_\ell(k\rho) = 0. \quad (48)$$

The k value satisfying Eq. (47), implies

$$TM: \quad J'_\ell(k\rho) = 0. \quad (49)$$

After obtaining all the fictitious values which occur in each method, it is found that once the method of integral formulation (either one of UT , LM , UL and TM methods) is adopted, the positions of fictitious values are independent of the type of boundary condition.

4.3. The Burton and Miller method

Burton and Miller⁴ proposed an integral equation by combining the UT and LM equations through an imaginary constant,

$$\left[U^i + \frac{i}{k} L^i \right] \{t\} = \left[T^i + \frac{i}{k} M^i \right] \{u\}. \quad (50)$$

Equation (50) is valid for all wave numbers, since $J_\ell(k\rho) + (i/k)J'_\ell(k\rho)$ is never zero for any value of k .

4.4. The dual BEM

By employing the UT and LM formulations to solve the exterior problem of acoustics, we have

$$[U^i] \{t\} = [T^i] \{u\}, \quad (51)$$

$$[L^i] \{t\} = [M^i] \{u\}. \quad (52)$$

A conventional approach to detect the nonunique solution is the criterion of satisfying both Eqs. (51) and (52) at the same time. The UT or LM method in conjunction with SVD

technique can extract out the fictitious frequencies. Employing the SVD technique, one can decompose Eq. (51) into

$$\Phi_T \Sigma_T \Psi_T^\dagger u = \Phi_U \Sigma_U \Psi_U^\dagger t, \quad (53)$$

where \dagger denotes the transpose conjugate, Φ_U , Ψ_U , Φ_T and Ψ_T are the unitary matrices, Σ_U and Σ_T are the diagonal matrices composed of the singular values $\sigma_i^{(U)}$ and $\sigma_i^{(T)}$ of U^i and T^i matrices, respectively. When k is a fictitious wave number (k_f^s), there exists a ϕ_s vector which satisfies

$$\begin{bmatrix} U^{i\dagger}(k_f^s) \\ T^{i\dagger}(k_f^s) \end{bmatrix} \phi_s = 0, \quad (54)$$

after using the Fredholm alternative theorem. Equation (54) is derived in Appendix A. By taking the transpose conjugate with respect to Eq. (54), we have

$$\phi_s^\dagger [U^i(k_f^s) \quad T^i(k_f^s)] = 0, \quad (55)$$

where ϕ_s is the fictitious boundary mode encountered in the ‘‘singular’’ equation. The assembly of U^i and T^i matrices in Eqs. (54) and (55) are found to be the SVD updating terms and documents, respectively. It is found that the fictitious modes can be extracted out from the left unitary matrix of U^i and T^i matrices.

Similarly, Eq. (52) can be rewritten as

$$\Phi_M \Sigma_M \Psi_M^\dagger u = \Phi_L \Sigma_L \Psi_L^\dagger t \quad (56)$$

where Φ_L , Ψ_L , Φ_M and Ψ_M are the unitary matrices, Σ_L and Σ_M are the diagonal matrices composed of the singular values $\sigma_i^{(L)}$ and $\sigma_i^{(M)}$ of L^i and M^i matrices, respectively. When k is a fictitious wave number (k_f^h), there exists a vector of ϕ_h which satisfies

$$\begin{bmatrix} L^{i\dagger}(k_f^h) \\ M^{i\dagger}(k_f^h) \end{bmatrix} \phi_h = 0, \quad (57)$$

after using the Fredholm alternative theorem. The derivation is the same as Eq. (54). By taking the transpose conjugate with respect to Eq. (57), we have

$$\phi_h^\dagger [L^i(k_f^h) \quad M^i(k_f^h)] = 0, \quad (58)$$

where ϕ_h is the fictitious mode encountered in the ‘‘hypersingular’’ equation. The assemble of L^i and M^i matrices in Eqs. (57) and (58) are found to be the SVD updating terms and documents, respectively. It is found that the fictitious boundary mode can be extracted out from the left unitary matrix of L^i and M^i matrices.

4.5. The CHIEF method

In order to solve the exterior acoustics in case of fictitious frequency, Schenck³ used the CHIEF method, which employed the boundary integral equations by collocating the interior point as an auxiliary constraint to promote the rank of influence matrix. Combination of the integral equations for the boundary points and those in the interior points yields an over-determined equation system,

$$\begin{bmatrix} U_{2N \times 2N}^B \\ U_{a \times 2N}^I \end{bmatrix} \{t\} = \begin{bmatrix} T_{2N \times 2N}^B \\ T_{a \times 2N}^I \end{bmatrix} \{\bar{u}\} \quad (59)$$

where the superscript B denotes collocation on the boundary, the superscript I denotes collocation on the interior domain and a is the number of additional interior points. Chen *et al.*⁵ suggested the optimum numbers and proper positions for the collocation points in the interior domain by using analytical study and numerical experiments.

5. Spurious Eigensolutions for Interior Problems using BEM

5.1. The complex-valued direct methods

By using the UT and LM formulations for the interior Dirichlet problem, we obtain the following equations,

$$[U^e]\{t\} = \{0\}, \quad (60)$$

$$[L^e]\{t\} = \{0\}. \quad (61)$$

The eigenequations are derived for the circular problem, respectively,

$$UT: \quad [J_\ell(k\rho) + iY_\ell(k\rho)]J_\ell(k\rho) = 0, \quad (62)$$

and

$$LM: \quad [J'_\ell(k\rho) + iY'_\ell(k\rho)]J_\ell(k\rho) = 0. \quad (63)$$

The true eigenvalues are the roots of $J_\ell(k\rho) = 0$ for the common part in the eigenequations of Eqs. (62) and (63).

For the interior Neumann problem, we obtain the following equations,

$$[T^e]\{u\} = \{0\}, \quad (64)$$

$$[M^e]\{u\} = \{0\}. \quad (65)$$

The eigenequations are derived, respectively,

$$UT: \quad [J_\ell(k\rho) + iY_\ell(k\rho)]J'_\ell(k\rho) = 0, \quad (66)$$

and

$$LM: \quad [J'_\ell(k\rho) + iY'_\ell(k\rho)]J'_\ell(k\rho) = 0. \quad (67)$$

The true eigenvalues are the roots of $J'_\ell(k\rho) = 0$ for the common part in the eigenequations of Eqs. (66) and (67).

5.2. The real-part direct methods

By employing the real-part kernels in *UT* and *LM* equations for the interior Dirichlet problem, we obtain the eigenequations,

$$UT: \quad Y_\ell(k\rho)J_\ell(k\rho) = 0, \quad \ell = 0, \pm 1, \pm 2, \dots, \pm(N-1), N, \quad (68)$$

$$LM: \quad Y'_\ell(k\rho)J_\ell(k\rho) = 0, \quad \ell = 0, \pm 1, \pm 2, \dots, \pm(N-1), N, \quad (69)$$

respectively. To satisfy Eqs. (68) and (69) at the same time, we obtain the true eigenequation ($J_\ell(k\rho) = 0$). Otherwise, they are spurious eigenequation ($Y_\ell(k\rho) = 0$ for *UT* method, $Y'_\ell(k\rho) = 0$ for *LM* method).

For the interior Neumann problem, we obtain the eigenequations,

$$UT: \quad Y_\ell(k\rho)J'_\ell(k\rho) = 0, \quad \ell = 0, \pm 1, \pm 2, \dots, \pm(N-1), N, \quad (70)$$

$$LM: \quad Y'_\ell(k\rho)J'_\ell(k\rho) = 0, \quad \ell = 0, \pm 1, \pm 2, \dots, \pm(N-1), N, \quad (71)$$

respectively. Similarly, it is easily found that $J'_\ell(k\rho) = 0$ is the true eigenequation and $Y_\ell(k\rho) = 0$ and $Y'_\ell(k\rho) = 0$ are spurious eigenequations using *UT* and *LM* approaches, respectively.

5.3. The imaginary-part direct methods

By employing the imaginary-part kernels in *UT* and *LM* equations for the interior Dirichlet problem, we obtain the eigenequations,

$$UT: \quad J_\ell(k\rho)J_\ell(k\rho) = 0, \quad \ell = 0, \pm 1, \pm 2, \dots, \pm(N-1), N, \quad (72)$$

$$LM: \quad J'_\ell(k\rho)J_\ell(k\rho) = 0, \quad \ell = 0, \pm 1, \pm 2, \dots, \pm(N-1), N, \quad (73)$$

respectively. To satisfy Eqs. (72) and (73) at the same time, we obtain the true eigenequation ($J_\ell(k\rho) = 0$). Otherwise, they are spurious eigenequation ($J_\ell(k\rho) = 0$ for *UT* method, $J'_\ell(k\rho) = 0$ for *LM* method).

For the interior Neumann problem, we obtain the eigenequations,

$$UT: \quad J_\ell(k\rho)J'_\ell(k\rho) = 0, \quad \ell = 0, \pm 1, \pm 2, \dots, \pm(N-1), N, \quad (74)$$

$$LM: \quad J'_\ell(k\rho)J'_\ell(k\rho) = 0, \quad \ell = 0, \pm 1, \pm 2, \dots, \pm(N-1), N, \quad (75)$$

respectively. Similarly, it is easily found that $J'_\ell(k\rho) = 0$ is the true eigenequation and $J_\ell(k\rho) = 0$ and $J'_\ell(k\rho) = 0$ are spurious eigenequations using *UT* and *LM* approaches, respectively.

5.4. The complex-valued indirect methods

By using the *UL* and *TM* formulations for the interior Dirichlet problem, we obtain the following equations,

$$[U^i]\{\phi\} = \{0\}, \quad (76)$$

$$[T^i]\{\psi\} = \{0\}. \quad (77)$$

The corresponding eigenequations are, respectively,

$$UL: \quad [J_\ell(k\rho) + iY_\ell(k\rho)]J_\ell(k\rho) = 0, \quad (78)$$

and

$$TM: \quad [J'_\ell(k\rho) + iY'_\ell(k\rho)]J_\ell(k\rho) = 0. \quad (79)$$

The true eigenvalues are the roots of $J_\ell(k\rho) = 0$ for the common part in the eigenequations of Eqs. (78) and (79).

For the interior Neumann problem, we can obtain the following equations,

$$[L^i]\{\phi\} = \{0\}, \quad (80)$$

$$[M^i]\{\psi\} = \{0\}. \quad (81)$$

The corresponding eigenequations are, respectively,

$$UL: \quad [J_\ell(k\rho) + iY_\ell(k\rho)]J'_\ell(k\rho) = 0, \quad (82)$$

and

$$TM: \quad [J'_\ell(k\rho) + iY'_\ell(k\rho)]J'_\ell(k\rho) = 0. \quad (83)$$

The true eigenvalues are the roots of $J'_\ell(k\rho) = 0$ for the common part in the eigenequations of Eqs. (82) and (83). If we employ the real-part or imaginary-part indirect BEM, we can obtain the true and spurious eigenvalues in a similar way. After comparing the real-part BEM and the imaginary-part BEM with the complex-valued BEM using either direct or indirect method, it can be realized that the reason why spurious eigenvalues occur is due to the loss of imaginary-part (real-part) constraints for the real-part BEM (imaginary-part BEM).

5.5. The dual BEM

The dual BEM in conjunction with SVD technique can also filter out the spurious eigen-solutions. Employing the SVD technique, we can decompose the real-part UT equation,

$$[T_R^e]\{u\} = [U_R^e]\{t\}, \quad (84)$$

into

$$\Phi_T \Sigma_T \Psi_T^T u = \Phi_U \Sigma_U \Psi_U^T t, \quad (85)$$

where the superscript T denotes the transpose and the subscript R denotes the real-part, and Φ is a left unitary matrix constructed by the left singular vectors, Σ is a diagonal matrix which has singular values allocated in a diagonal line, and Ψ^T is the transpose of a right unitary matrix constructed by the right unitary vectors. Similarly, the real-part LM equation,

$$[M_R^e]\{u\} = [L_R^e]\{t\} \quad (86)$$

can be rewritten as

$$\Phi_M \Sigma_M \Psi_M^T u = \Phi_L \Sigma_L \Psi_L^T t. \quad (87)$$

When k is a true eigenvalue, there exists a true boundary mode $\tilde{\psi}$ satisfying

$$\begin{bmatrix} U_R^e \\ L_R^e \end{bmatrix} \tilde{\psi}_D = 0, \text{ for the Dirichlet problem} \quad (88)$$

or

$$\begin{bmatrix} T_R^e \\ M_R^e \end{bmatrix} \tilde{\psi}_N = 0, \text{ for the Neumann problem} \quad (89)$$

after assembling Eqs. (85) and (87), where $\tilde{\psi}_D$ and $\tilde{\psi}_N$ are the true boundary modes for the Dirichlet and Neumann problems, respectively. It is found that true boundary modes can be extracted out from the right unitary vectors of U_R^e and L_R^e , or T_R^e and M_R^e .

If k is a spurious eigenvalue, there exists a spurious boundary mode $\tilde{\phi}$ satisfying

$$\tilde{\phi}_s^T [U_R^e \quad T_R^e] = 0, \quad (90)$$

after using the Fredholm alternative theorem. The derivation is shown in Appendix B. After transposing Eq. (90), we have

$$\begin{bmatrix} U_R^{eT} \\ T_R^{eT} \end{bmatrix} \tilde{\phi}_s = 0. \quad (91)$$

Similarly, we have

$$\tilde{\phi}_h^T [L_R^e \quad M_R^e] = 0 \quad \text{or} \quad \begin{bmatrix} L_R^{eT} \\ M_R^{eT} \end{bmatrix} \tilde{\phi}_h = 0 \quad (92)$$

where $\tilde{\phi}_s$ and $\tilde{\phi}_h$ are the spurious boundary modes encountered in the singular (UT) and hypersingular (LM) equations, respectively. It is found that the spurious boundary modes can be extracted out from the left unitary vectors of U_R^e and T_R^e , or L_R^e and M_R^e matrices, respectively.

5.6. The CHEEF methods

Chen *et al.*²⁰ extended the CHIEF to CHEEF method by combining the integral equations for the boundary points and those in the exterior points. It yields the over-determined equation system,

$$\begin{bmatrix} U_{2N \times 2N}^B \\ U_{a \times 2N}^E \end{bmatrix} \{t\} = 0 \quad (93)$$

or

$$\begin{bmatrix} T_{2N \times 2N}^B \\ T_{a \times 2N}^E \end{bmatrix} \{u\} = 0, \quad (94)$$

for the Dirichlet and Neumann problems, respectively. The superscript E denotes collocation on the exterior domain. It can filter out the spurious eigensolutions efficiently for the interior problem in a similar way of CHIEF for the exterior problems.

6. Numerical Examples

Case 1. Fictitious values for an exterior acoustic problem subject to the Neumann boundary condition.

For the first example, we consider the Neumann problem (nonuniform radiation of an infinite circular cylinder with a radius of $a = 1.0$ m). This problem was chosen because the exact solution is known.²⁴ The Neumann boundary condition is applied to the cylinder surface. The portion ($-\alpha < \theta < \alpha$) is assigned a unit value, while the remaining portion is assigned a homogeneous value. The exact solution is given by

$$u(r, \theta) = -\frac{2}{\pi k} \sum_{n=0}^{\infty} \imath \frac{\sin(n\alpha)}{n} \frac{H_n^{(1)}(kr)}{H_n^{(1)}(ka)} \cos(n\theta), \quad r \geq a, \quad 0 \leq \theta < 2\pi, \quad (95)$$

where the former symbol “ \imath ” denotes the Neumann factor, the $H_n^{(1)}$ and $H_n^{\prime(1)}$ denote the first kind Hankel functions with order n and its derivative, respectively. Thirty-two elements are adopted in the BEM mesh and α is chosen as $\pi/9$ for this case. Using the singular (UT)

equation, the positions where the irregular values occur can be found in Fig. 5 for the solution $u(a, 0; k)$ versus ka . It is found that irregular values occur at the positions of $J_{n,m}$, which is the m th zero of $J_n(ka)$. It agrees well as predicted in Eq. (36). Figure 6 shows the solution $u(a, 0; k)$ versus ka using the hypersingular (LM) equation, the positions where

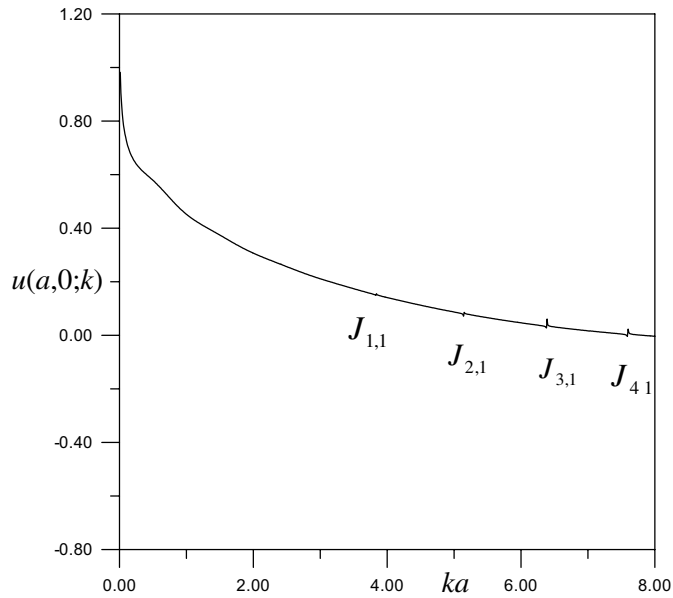


Fig. 5. The potential of $u(a, 0; k)$ versus ka using the UT method.

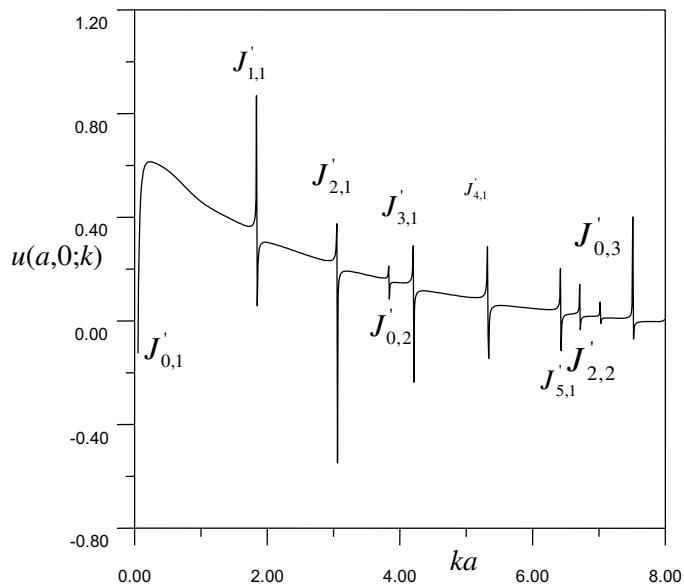


Fig. 6. The potential of $u(a, 0; k)$ versus ka using the LM method.

the irregular values occur at the positions of $J'_{n,m}$, which is the m th zero of $J'_n(ka)$. It also agrees well as predicted in Eq. (37). Figure 7 shows the solution $u(a, 0; k)$ versus ka using the Burton and Miller approach. Figure 8 shows the solution $u(a, 0; k)$ versus ka using the CHIEF method. Both of these methods can avoid the unstable solution near the irregular

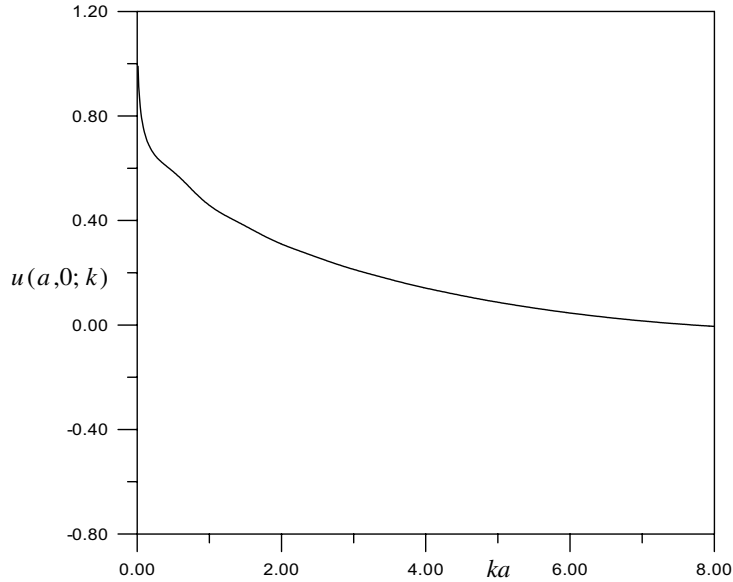


Fig. 7. The potential of $u(a, 0; k)$ versus ka using the Burton and Miller method.

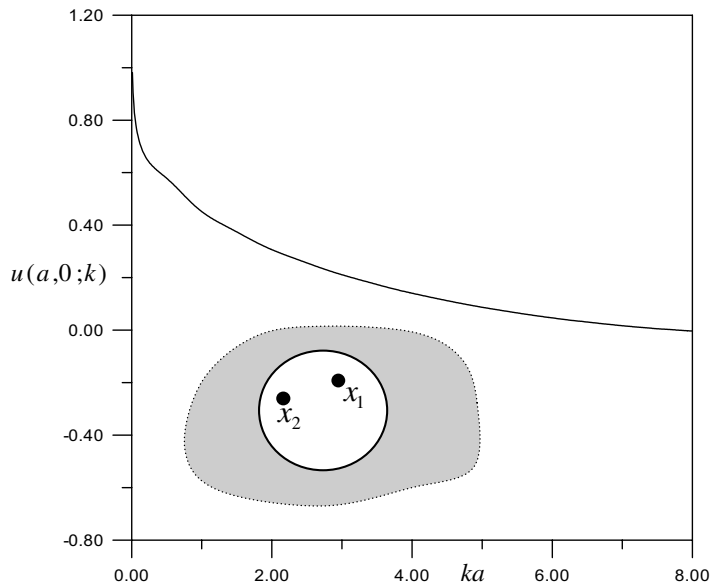


Fig. 8. The potential of $u(a, 0; k)$ versus ka using the CHIEF method.

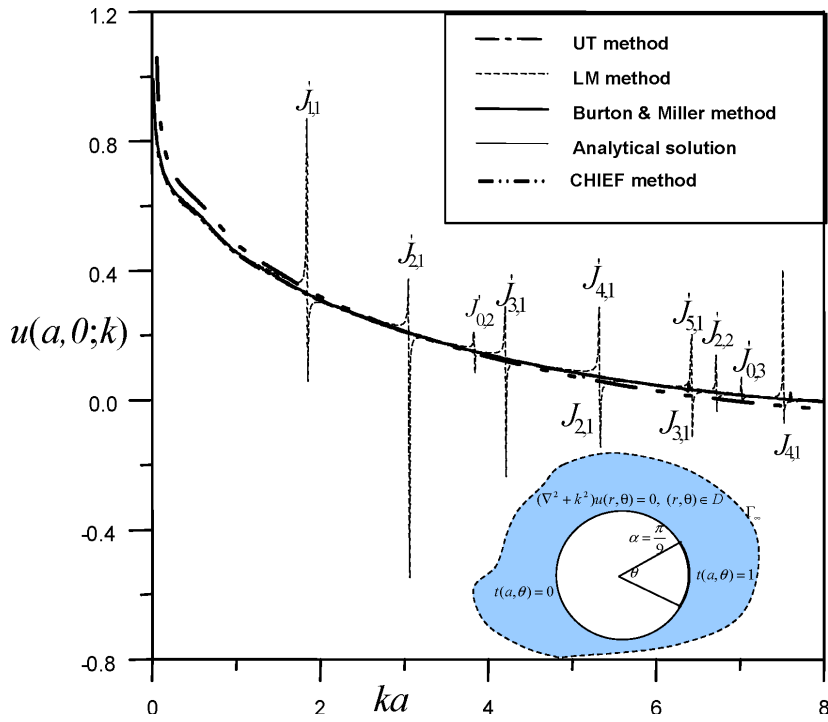


Fig. 9. The potential of $u(a, 0; k)$ versus ka using different methods.

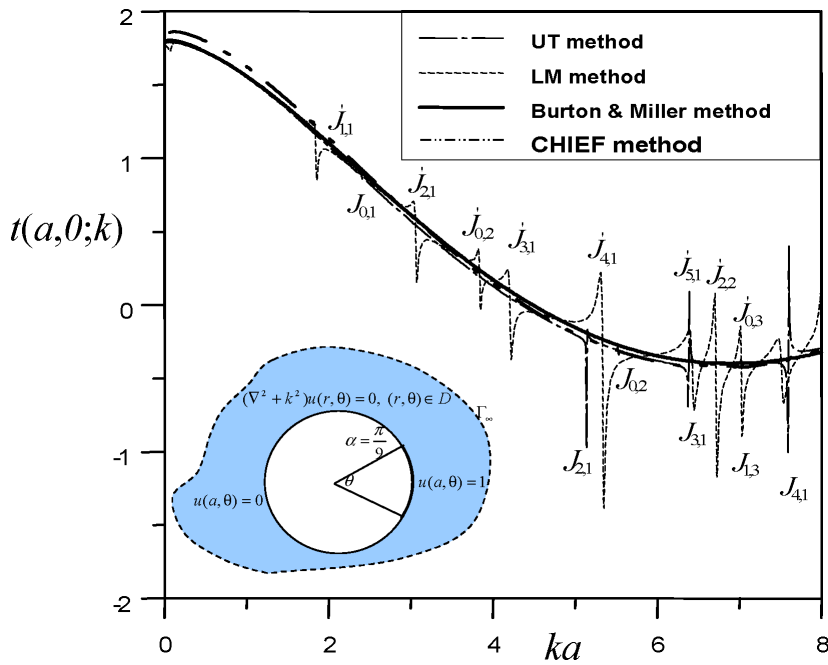


Fig. 10. The potential of $t(a, 0; k)$ versus ka using different methods.

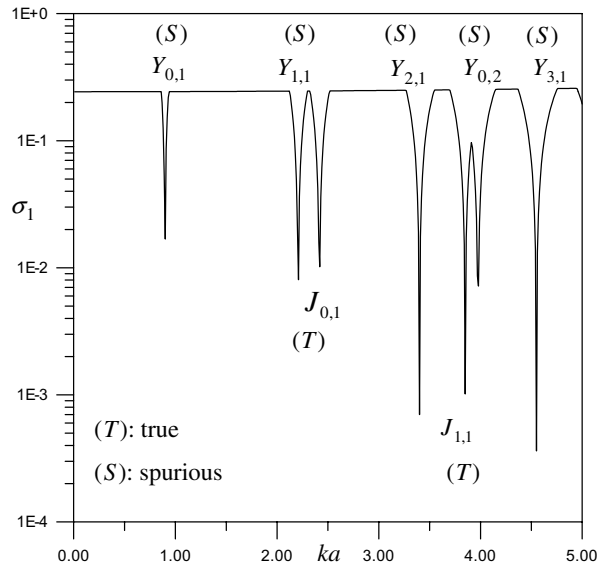


Fig. 11. The minimum singular value σ_1 versus ka using the real-part BEM.

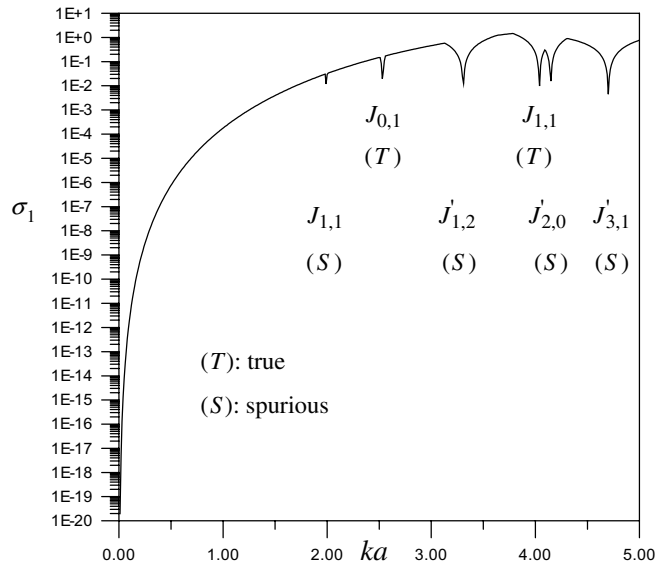


Fig. 12. The minimum singular value σ_1 versus ka using the imaginary-part BEM.

wave numbers. The results of the analytical solution, the *UT* method, the *LM* method, Burton and Miller approach, and CHIEF method are all shown in Fig. 9.

Case 2. Fictitious values for an exterior acoustic problem subject to the Dirichlet boundary condition.

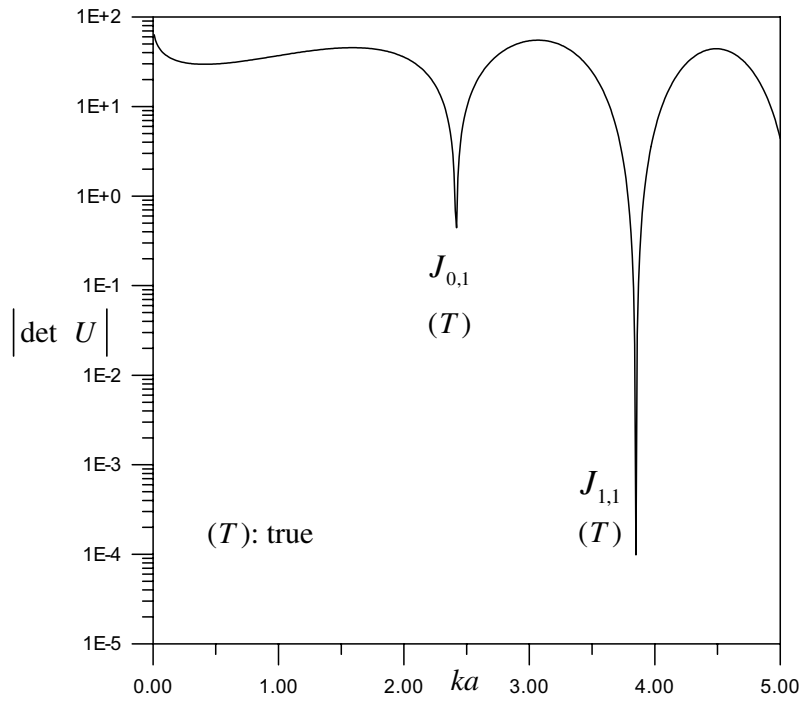


Fig. 13. The absolute value of determinant versus ka using the complex-valued BEM.

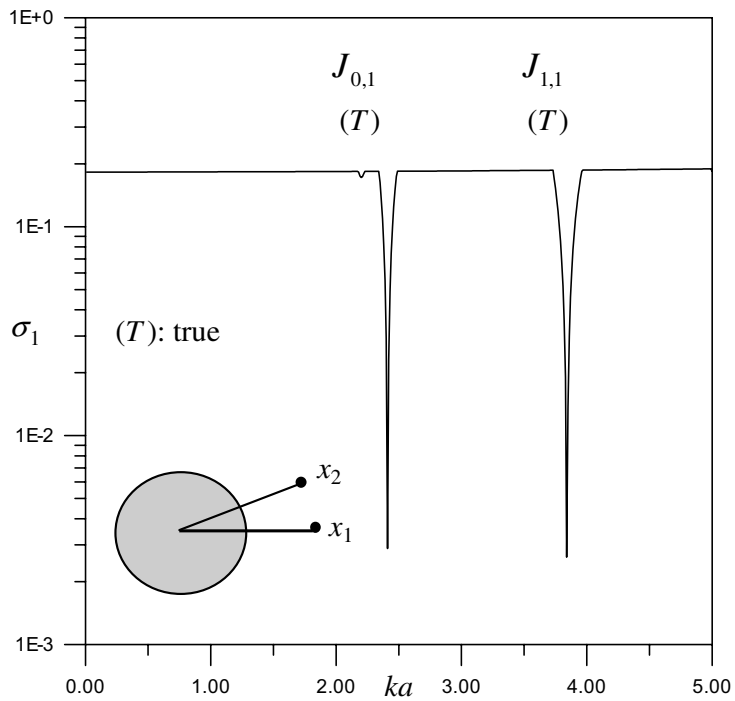


Fig. 14. The minimum singular value σ_1 versus ka using the CHEEF method.

In order to clarify how the irregular frequencies depend on the types of boundary conditions, the second problem subject to the Dirichlet boundary condition is designed. The analytical solution is

$$u(r, \theta) = \frac{2}{\pi} \sum_{n=0}^{\infty} \frac{\sin(n\alpha)}{n} \frac{H_n^{(1)}(kr)}{H_n^{(1)}(ka)} \cos(n\theta), \quad r \geq a, \quad 0 \leq \theta < 2\pi. \quad (96)$$

Figure 10 shows the solution $u(a, 0; k)$ versus ka using the *UT* method, the *LM* method, Burton and Miller approach and CHIEF method. It is found that the irregular frequencies in Fig. 10 occur at the same positions in comparison with those of Fig. 9. This confirms the conclusion that the irregular values depend on the integral formulation instead of the types of boundary conditions (Dirichlet or Neumann).

Case 3. Spurious eigensolution for an interior acoustic problem.

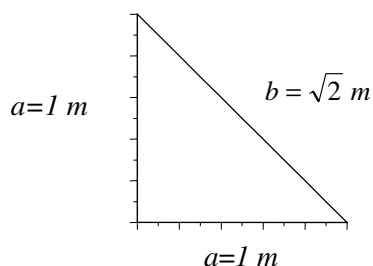


Fig. 15. Right triangle domain.

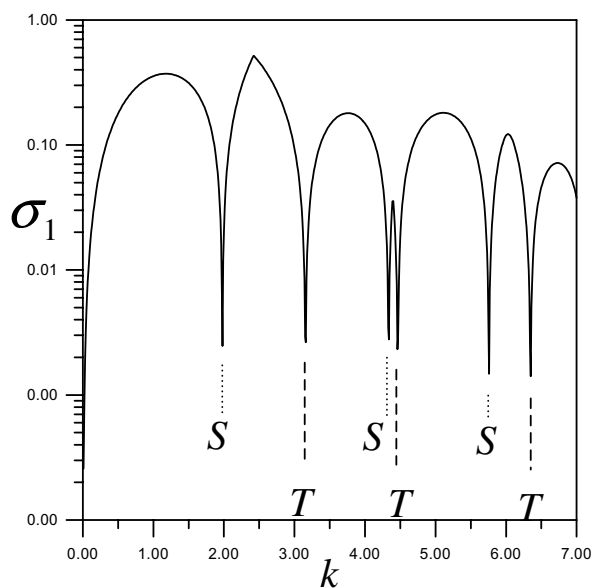


Fig. 16. The first minimum singular values σ_1 versus k of a right triangle cavity using the real-part *UT* equation subject to Neumann boundary conditions.

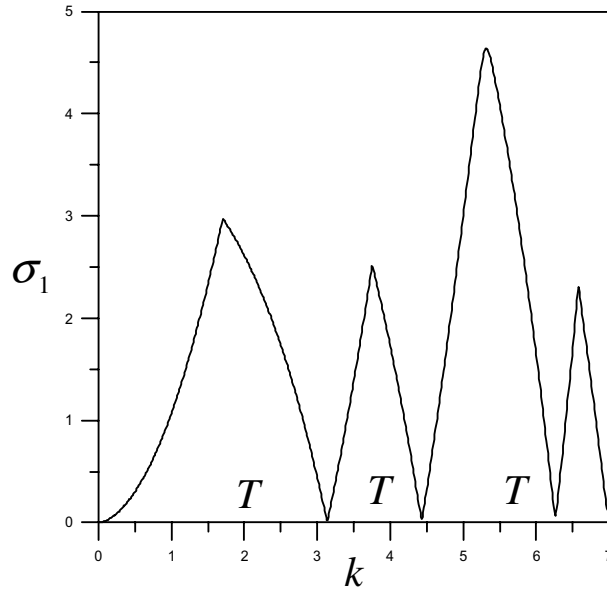
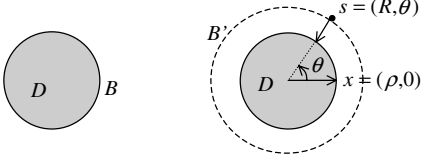
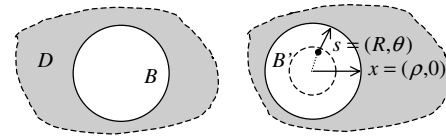


Fig. 17. The first minimum singular value for different wave number using the SVD updating technique.

We considered a circular cavity with a radius 1.0 m subjected to the Dirichlet boundary condition. Figure 11 shows the first minimum singular value, σ_1 , versus ka , where the true and spurious eigenvalues are obtained if only the real-part UT equation is used. In the range of $0 < ka < 5$, we have two true eigenvalues ($J_{0,1}(2.405)$ and $J_{1,1}(3.832)$) and five spurious eigenvalues ($Y_{0,1}(0.894)$, $Y_{1,1}(2.197)$, $Y_{2,1}(3.384)$, $Y_{0,2}(3.958)$ and $Y_{3,1}(4.527)$), where $Y_{n,m}$ is the m th zero of $Y_n(ka)$. It agrees well as predicted in Eq. (68). Figure 12 shows the first minimum singular value, σ_1 , versus ka , where the true and spurious eigenvalues are obtained if only imaginary-part LM equation is used. Only ten elements are adopted in the BEM mesh to avoid the ill-conditioned behavior. We have two true eigenvalues ($J_{0,1}(2.405)$ and $J_{1,1}(3.832)$) and four spurious eigenvalues ($J'_{1,1}(1.841)$, $J'_{2,1}(3.054)$, $J'_{0,2}(3.832)$ and $J'_{3,1}(4.201)$). It also agrees well as predicted in Eq. (73). Figure 13 shows the absolute value of determinant versus ka using the complex-valued UT equation, where only true eigenvalues are obtained. Figure 14 shows the first minimum singular value, σ_1 , versus ka , using the CHEEF method where only the true eigenvalues are obtained.

Case 4. We consider a right triangle problem subjected to the Neumann boundary condition with $a = 1$ m and $b = \sqrt{2}$ m is shown in Fig. 15 for a case of general geometry. The exact eigenvalues are known¹⁰ to be $n\pi$, $n\sqrt{2}\pi$ for $n = 1, 2, \dots$. Thirty elements in the BEM mesh were adopted. Figure 16 indicates the first minimum singular value, σ_1 versus k , where the true and spurious eigenvalues can be obtained. In the range of $0 < k < 7$, we have the three true eigenvalues (3.14, 4.47 and 6.34) and three spurious eigenvalues (1.98, 4.34 and 5.76). Figure 17 shows the first minimum singular value versus different wave number using the SVD updating technique, then all the spurious eigenvalues are filtered out.

Table 2. The relationship between the spurious eigensolution (interior problem) and fictitious solution (exterior problem) using the indirect.

		Problem type								
		Interior problem			Exterior problem					
										
		Method						Method		
		Real-part BEM		Imag.-part ⁸ BEM		Complex-Valued BEM		Singular layer approach	Double layer approach	
Equation		<i>UL</i>	<i>TM</i>	<i>UL</i>	<i>TM</i>	<i>UL</i>	<i>TM</i>	<i>UL</i>	<i>TM</i>	
Dirichlet B.C. analytical spurious eigenequation		Y_n	Y'_n	J_n	J'_n	\times	\times	Dirichlet B.C. analytical fictitious solution	J_n	J'_n
Neumann B.C. analytical spurious eigenequation		Y_n	Y'_n	J_n	J'_n	\times	\times	Neumann B.C. analytical fictitious solution	J_n	J'_n

7. Conclusions

In this paper, the mechanism of fictitious values and spurious eigenvalues in BEM was investigated using the degenerate kernels and circulants for a discrete system of a circular domain. The reason why spurious eigenvalues occur in the real-part or imaginary-part BEM and why fictitious frequencies appear in the integral formulation results from the rank deficiency of influence matrix. The numerical results agree well with the analytical prediction. SVD updating technique can study the spurious eigenvalues and fictitious frequencies in a unified manner. The relationship between spurious eigenvalues of interior problem and fictitious values of exterior problem using the direct and indirect methods was summarized in Table 1 and Table 2, respectively. It is interesting to note that the true boundary modes for interior problem can be found from the right unitary vector of SVD, while the spurious or fictitious boundary modes can be extracted from the left unitary vector. The similarities of CHIEF and CHEEF methods were also explored.

Acknowledgment

Financial support from the National Science Council, under Grant No. NSC 94-2115-M-019-003, for National Taiwan Ocean University is gratefully acknowledged.

Appendix A

For the exterior radiation problem subject to the Dirichlet boundary condition ($u(\mathbf{x}) = \bar{u}$), Eq. (51) reduces to

$$[U^i]\{t\} = [T^i]\{\bar{u}\} = \{b\}. \quad (\text{A.1})$$

In case of a fictitious frequency, $[U^i]$ is singular. According to the Fredholm alternative theorem, $\{t\}$ has a solution if and only if $\{b\}$ satisfies

$$\{b^\dagger\}\phi_s = 0, \quad (\text{A.2})$$

where ϕ_s is a nontrivial solution for the adjoint system such that

$$[U^{i\dagger}]\phi_s = 0. \quad (\text{A.3})$$

By substituting Eq. (A.1) into Eq. (A.2), we have

$$\{\bar{u}^\dagger\}[T^{i\dagger}]\phi_s = 0. \quad (\text{A.4})$$

Since \bar{u} can be arbitrary, Eq. (A.4) implies

$$[T^{i\dagger}]\phi_s = 0. \quad (\text{A.5})$$

By assembling Eq. (A.3) and Eq. (A.5) together, we can construct

$$\begin{bmatrix} U^{i\dagger} \\ T^{i\dagger} \end{bmatrix} \phi_s = 0. \quad (\text{A.6})$$

By taking the transpose conjugate with respect to Eq. (A.6), we have

$$\phi_s^\dagger [U^i \quad T^i] = 0. \quad (\text{A.7})$$

The T^i matrix can be seen as the updating document with U^i in Eq. (A.7), while the $T^{i\dagger}$ matrix is the updating term with $U^{i\dagger}$ in Eq. (A.6).

Appendix B

To filter out the spurious eigenvalues, a nonhomogeneous boundary excitation is considered by

$$[U_R^e]\{t\} = [T_R^e]\{u\} = \{b\}, \quad (\text{B.1})$$

where $\{u\}$ or $\{t\}$ are boundary excitation sources. Since spurious eigenvalues are embedded in both the Dirichlet and Neumann problems, we have

$$\{b\}^T \tilde{\phi}_s = 0 \quad (\text{B.2})$$

where $\tilde{\phi}_s$ satisfies

$$[U_R^e]^T \tilde{\phi}_s = 0, \quad \text{for the Dirichlet problem,} \quad (\text{B.3})$$

$$[T_R^e]^T \tilde{\phi}_s = 0, \quad \text{for the Neumann problem,} \quad (\text{B.4})$$

according to the Fredholm alternative theorem. By substituting Eq. (B.1) into Eq. (B.2), we have

$$u^T [T_R^e]^T \tilde{\phi}_s = 0, \quad \text{for the Dirichlet problem,} \quad (\text{B.5})$$

$$t^T [U_R^e]^T \tilde{\phi}_s = 0, \quad \text{for the Neumann problem.} \quad (\text{B.6})$$

Since u and t can be arbitrary for the Dirichlet and Neumann problems, respectively, we have

$$[T_R^e]^T \tilde{\phi}_s = 0, \quad \text{for the Dirichlet problem,} \quad (\text{B.7})$$

$$[U_R^e]^T \tilde{\phi}_s = 0, \quad \text{for the Neumann problem.} \quad (\text{B.8})$$

By combining Eq. (B.3) with (B.7), we have

$$\begin{bmatrix} U_R^T \\ T_R^T \end{bmatrix} \tilde{\phi}_s = 0. \quad (\text{B.9})$$

Similarly, Eq. (B.9) can be obtained by combined Eq. (B.4) with (B.8).

References

1. J. T. Chen, On fictitious frequencies using dual series representation, *Mech. Res. Comm.* **25**(5) (1998) 529–534.
2. J. T. Chen and S. R. Kuo, On fictitious frequencies using circulants for radiation problems of a cylinder, *Mech. Res. Comm.* **27**(3) (2000) 49–58.
3. H. A. Schenck, Improved integral formulation for acoustic radiation problems, *J. Acoust. Soc. Am.* **44**(1) (1976) 41–58.
4. A. J. Burton and G. F. Miller, The application of integral equation methods to numerical solutions of some exterior boundary value problem, *Proc. Royal Society London Ser. A* **323** (1971) 201–210.
5. I. L. Chen, J. T. Chen and M. T. Liang, Analytical study and numerical experiments for radiation and scattering problems using the CHIEF method, *J. Sound Vib.* **248**(5) (2001) 809–828.
6. J. T. Chen and K. H. Chen, Dual integral formulation for determining the acoustic modes of a two-dimensional cavity with a degenerate boundary, *Engng. Anal. Bound. Elem.* **21**(2) (1998) 105–116.
7. A. J. Nowak and A. C. Neves (eds.), *Multiple Reciprocity Boundary Element Method* (Comp. Mech. Publ., Southampton, 1994).
8. G. De Mey, A simplified integral equation method for the calculation of the eigenvalues of Helmholtz equation, *Int. J. Numer. Meth. Engng.* **11** (1977) 1340–1342.
9. J. T. Chen, S. R. Kuo and K. H. Chen, A nonsingular integral formulation for the Helmholtz eigenproblems of a circular domain, *J. Chinese Institute Engineers* **22**(6) (1999) 729–739.
10. G. R. G. Tai and R. P. Shaw, Helmholtz equation eigenvalues and eigenmodes for arbitrary domains, *J. Acoust. Soc. Am.* **56** (1974) 796–804.
11. J. T. Chen and F. C. Wong, Analytical derivations for one-dimensional eigenproblems using dual BEM and MRM, *Engng. Anal. Bound. Elem.* **20**(1) (1997) 25–33.
12. N. Kamiya, E. Andoh and K. Nogae, A new complex-valued formulation and eigenvalue analysis of the Helmholtz equation by boundary element method, *Adv. Engng. Soft.* **26** (1996) 219–227.

13. W. Yieh, J. T. Chen, K. H. Chen and F. C. Wong, A study on the multiple reciprocity method and complex-valued formulation for the Helmholtz equation, *Adv. Engng. Soft.* **29**(1) (1997) 1–6.
14. S. W. Kang, J. M. Lee and Y. J. Kang, Vibration analysis of arbitrarily shaped membranes using non-dimensional dynamic influence function, *J. Sound Vib.* **221**(1) (1999) 117–132.
15. J. T. Chen, S. R. Kuo, K. H. Chen and Y. C. Cheng, Comments on vibration analysis of arbitrary shaped membranes using nondimensional dynamic influence function, *J. Sound Vib.* **234**(1) (2000) 156–171.
16. S. W. Kang and J. M. Lee, Eigenmode analysis of arbitrarily shaped two dimensional cavities by the method of point-matching, *J. Acoust. Soc. Am.* **107** (2000) 1153–1160.
17. W. Schroeder and I. Wolff, The origin of spurious modes in numerical solutions of electromagnetic field eigenvalue problems, *IEEE Transaction on Microwave Theory and Techniques* **42**(4) (1994) 644–653.
18. J. R. Chang, W. Yieh and J. T. Chen, Determination of natural frequencies and natural mode of a rod using the dual BEM in conjunction with the domain partition technique, *Comput. Mech.* **24**(1) (1999) 29–40.
19. J. T. Chen, C. X. Huang and K. H. Chen, Determination of spurious eigenvalues and multiplicities of true eigenvalues using the real-part dual BEM, *Comput. Mech.* **24**(1) (1999) 41–51.
20. I. L. Chen, J. T. Chen, S. R. Kuo and M. T. Liang, Analytical study and numerical experiments for true and spurious eigensolutions of arbitrary cavities using the combined Helmholtz exterior integral equation formulation method, *J. Acoust. Soc. Am.* **109**(3) (2001) 982–999.
21. M. W. Berry, Z. Dramč and E. R. Jrssup, Matrices, vector spaces, and information retrieval, *SIAM Review* **41**(2) (1999) 335–362.
22. P. A. Ramachandran, Method of fundamental solutions: Singular value decomposition analysis, *Comm. Numer. Meth. Engng.* **18** (2002) 789–801.
23. D. I. Witter and M. W. Berry, DOWDATING the latent semantic indexing model for conceptual information retrieval, *J. Comput.* **41**(8) (1998) 589–601.
24. I. Harari, P. E. Barbone, M. Slavutin and R. Shalom, Boundary infinite elements for the Helmholtz equation in exterior domains, *Int. J. Numer. Meth. Engng.* **41** (1998) 1105–1131.